www.czasopisma.pan.pl PAN POLSKA AKADEMIA NAUK www.journals.pan.pl

PAN ARCHIVES OF ACOUSTICS
Vol. **43**, No. 4, pp. 681–687 (2018)

DOI: 10.24425/aoa.2018.125161

Mixed Pseudo-orthogonal Frequency Coding for SAW RFID Tags

Mengru XU, Xia XIAO, Qing YUAN, Yong ZONG

Key Laboratory of Imaging and Sensing Microelectronic Technology
School of Electronics, Tianjin University
Tianjin 300072, China; e-mail: xiaxiao@tju.edu.cn

(*received April 6, 2017; accepted May 24, 2018*)

A mixed pseudo-orthogonal frequency coding (Mixed-POFC) structure is proposed as a new spread-spectrum technique in this paper, which employs frequency and time diversity to enhance tag properties and balances the spectrum utilization and code diversity. The coding method of SAW RFID tags in this paper uses Mixed-POFC with multi-track chip arrangements. The cross-correlation and auto correlation of Mixed-POFC and POFC are calculated to demonstrate the reduced overlap between the adjacent center frequencies with the Mixed-POFC method. The center frequency of the IDT and Bragg reflectors is calculated by a coupling of modes (COM) module. The combination of the calculation results of the Bragg reflectors shows that compared with a 7-chip POFC, the coding number of a 7-chip Mixed-POFC is increased from 120 to 144 with the same fractional bandwidth of 12%. To demonstrate the validity of Mixed-POFC, finite element analysis (FEA) technology is used to analyze the frequency characteristics of Mixed-POFC chips. The maximum error between designed frequencies and simulation frequencies is only 1.7%, which verifies that the Mixed-POFC method is feasible.

Keywords: SAW RFID tag; OFC; POFC; Mixed-POFC; COMSOL.

1. Introduction

SAW RFID has attracted much attention due to its many advantages, such as a wide temperature range, passive operation, reliability and maintenance-free life cycle (Wilson *et al.*, 2009; Plessky *et al.*, 1995). Several methods – such as PSK coding, delay line coding and time position coding (Plessky *et al.*, 1995) have been invented to code SAW RFID tags. Using those methods, anti-jamming capabilities have been generally enhanced and the coding capacity has been expanded on the order of 10^6. However, the size of chip is still relatively large, and the coding capacity can still be expanded in some degree. After the development of OFC (Malocha *et al.*, 2004) and POFC (Saldanha, Malocha, 2012) researchers have attempted to apply this concept to SAW RFID systems (Liu *et al.*, 2016; Humphries, Malocha, 2015; Humphries *et al.*, 2015; Rodriguez *et al.*, 2014; Malocha *et al.*, 2014). OFC and POFC SAW tags use short-serial Bragg reflectors to reflect a particular frequency. Coding is hidden in the center frequency and time-delay of the reflected signal. Generally, there exist two methods to increase coding diversity. The first one is increasing the chip length. However, an OFC SAW tag is usually limited to a very small size – longer length of chips causes more energy storage (Saldanha, Malocha, 2008) and greater attenuation of SAW. The second one is improving the coding method (Gallagher, Malocha, 2013).

In this paper, a Mixed-POFC coding method is proposed in which the fractional bandwidth is dramatically decreased while the coding diversity is increased. Meanwhile, the coding method avoids the overlap between two adjacent chips when keeping chips to a relatively small size. The Mixed-POFC SAW devices can be used in communication, sensor and RFID tag applications.

The following sections are organized as follows: the theory of OFC and POFC are introduced in Sec. 2. In Sec. 3, the details of Mixed-POFC and the advantages of this coding method are presented. The COM module of chips are numerically computed to show the transfer response of chips in frequency and time domain, respectively. The development of a tag model using FEA technology is also introduced in this section. Analysis and discussion are summarized in Sec. 4.

2. OFC and pseudo-OFC

2.1. OFC

Orthogonal frequency coding in SAW devices was first proposed in 2004 (Puccio *et al.*, 2004). An OFC SAW tag is shown in Fig. 1. The wideband IDT transforms energy between voltage and surface waves. The chips carry the coding information, including the center frequency and time delay. The ideal time domain transfer function of an OFC device is defined as:

$$h_{\mathrm{OFC}}(t) = \sum_{i=1}^{N_c} a_i \cdot \mathrm{rect}\left[\frac{t-\tau_{p_i}}{\tau_{\mathrm{chip}}}\right] \cos[2\pi f_{\mathrm{chip}_i}(t-\tau_{p_i})], \quad (1)$$

where $\mathrm{rect}(t)$ represents the rectangular envelope of ideal signal response, N_c is the number of chips, a_i is the weighting coefficient of the i-th chip, f_{chip_i} is the center frequency of the i-th chip, τ_{p_i} is the time delay from the IDT to the i-th chip, and τ_{chip} is the chip length. According to OFC theory, the parameter τ_{chip} is constant. The relationship between $f_{\mathrm{chip_i}}$ and τ_{chip} is defined as

$$f_{\mathrm{chip}_i} \cdot \tau_{\mathrm{chip}} = M_i, \quad (2)$$

where M_i must be an integer number of half the wavelength at f_{chip_i}. The center frequency of each chip is spaced $\tau_{\mathrm{chip}}^{-1}$ apart in the frequency domain from the adjacent-frequency chips:

$$f_{\mathrm{chip}_i} = f_o + \frac{C_i}{\tau_{\mathrm{chip}}}, \quad (3)$$

where f_o is the carrier frequency, and $C_i (C = 0, \pm 1, \pm 2, \pm 3\mathrm{L})$ is the center frequency of the i-th chip apart from the carrier frequency.

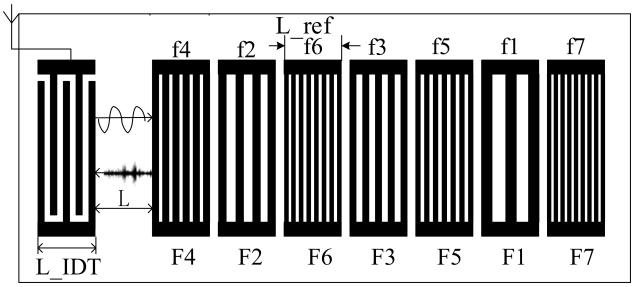

Fig. 1. A SAW OFC RFID tag with 7 chips with different center frequencies.

As an example of an ideal transfer function for OFC, τ_{chip} is defined as $50/f_0$ in terms of the YZ-$LiNbO_3$ substrate, and the null of a chip is chosen as the peak of the adjacent one in frequency domain, seen in Fig. 2. The frequency axis is normalized to the center frequency. The fractional bandwidth is 12%, which is calculated by the difference between the upper frequency and the lower frequency. The overlap between first adjacent (f_1 and f_2) frequencies is large, while the overlap between second (f_1 and f_3) adjacent frequencies is small.

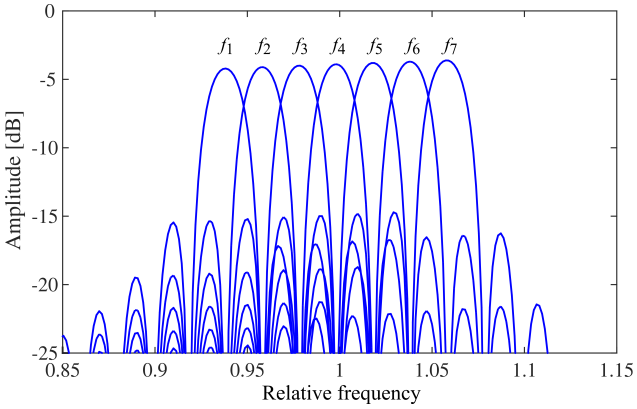

Fig. 2. The frequency response of a 7-chip OFC system.

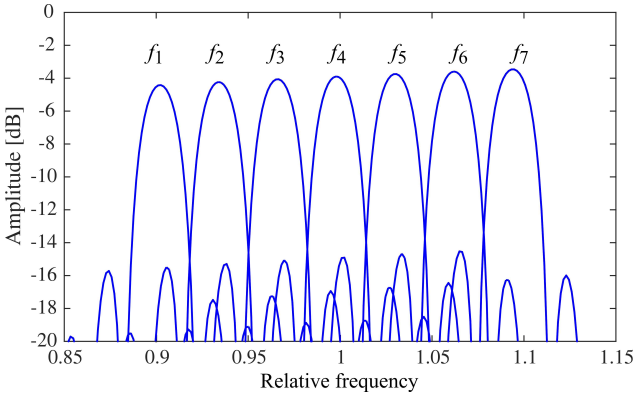

Fig. 3. The frequency response of a 7-chip POFC ($S = 1.6$) system.

2.2. Pseudo-OFC

To improve the performance of OFC SAW RFID, the center frequencies of each chip have been changed to reduce the cross-correlation between adjacent chips. For pseudo-orthogonal frequency coding,

$$f_{\mathrm{chip}_i} = f_0 + S \cdot \frac{C_i}{\tau_{\mathrm{chip}}}, \quad (4)$$

where the S parameter is the frequency spacing factor chosen based on correlation properties of an individual chip. The value of the S parameter is always defined as 1.6 or 2.4 (Malocha *et al.*, 2014).

As an example of ideal transfer function of POFC, τ_{chip} is defined as $50/f_0$ in terms of the YZ-$LiNbO_3$ substrate, and the frequency axis is normalized to center frequency. The fractional bandwidth is 19.2%. Although most of the overlap between adjacent (f_1 and f_2) frequencies has been avoided, some overlap still exists below −14 dB in the main lobe. As seen in Fig. 2 (OFC system) and Fig. 3 (POFC system), though the overlap is decreased, the cost of the fractional bandwidth is increased from 12% in the OFC to 19.2% in the POFC at the same center frequency.

POFC has successfully solved the problem of non-ideal OFC responses: the overlap of adjacent chips in

the frequency domain is decreased. However, with the increase of the S parameter, the cross-correlation has a significant decrease while the cost of bandwidth is increased. As an example, the fractional bandwidth increases from 12% to 19.2% for 7-chip OFC and 7-chip pseudo-OFC (S = 1.6) systems with an average of 50 electrodes for each reflector, respectively. However, if the OFC technique is still used, a 9-chip system can be built with the same fractional bandwidth, which means the coding diversity can be 72 times greater than before. If S = 2.4, the situation can be even worse.

As shown in Fig. 2, the overlap between adjacent chip frequencies is large (e.g., f_1 and f_2), but the overlap between alternate chip frequencies is small (e.g., f_1 and f_3). This frequency characteristic is shown by computing the correlation.

As one of the most important parameters of the OFC SAW RFID tag system, the cross-correlation of two chips and auto-correlation of a single chip are represented by time-limited functions $f(t)$ and $g(t)$, which can be obtained by (Stremler, 1990)

$$R_f(\tau) = \int_{-T/2}^{T/2} f(t)f(t-\tau)\,\mathrm{d}t, \tag{5}$$

$$R_{fg}(\tau) = \int_{-T/2}^{T/2} f(t)g(t-\tau)\,\mathrm{d}t, \tag{6}$$

and, if the two chips are orthogonal

$$\int_{-T/2}^{T/2} f(t)g(t-\tau)\,\mathrm{d}t = \begin{cases} 1, & \text{if} \quad g(t) = f(t), \\ 0, & \text{otherwise.} \end{cases} \tag{7}$$

The level of correlation for chips is quantified using auto- and cross-correlation parameters. There is a considerable reduction in the correlation peaks for chips having different center frequencies. The wider the spacing of the center frequencies is, the lower the value of the cross-correlation becomes, which demonstrates the smaller overlap between the adjacent center frequencies.

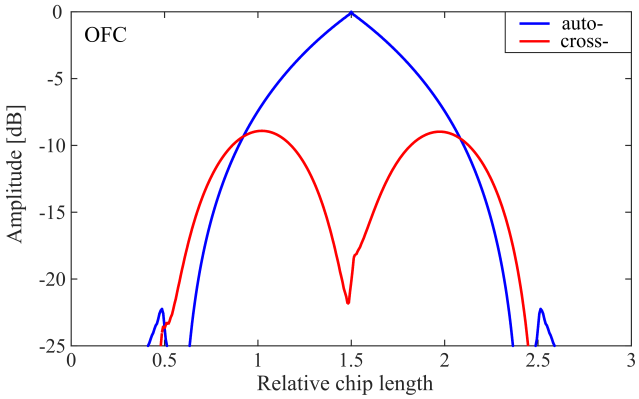

Fig. 4. COM simulation of auto- and cross-correlation of OFC. The time axis is normalized with chip length τ_{chip}. The cross-correlation between adjacent frequencies is shown by the dotted line with peak values of −9 dB.

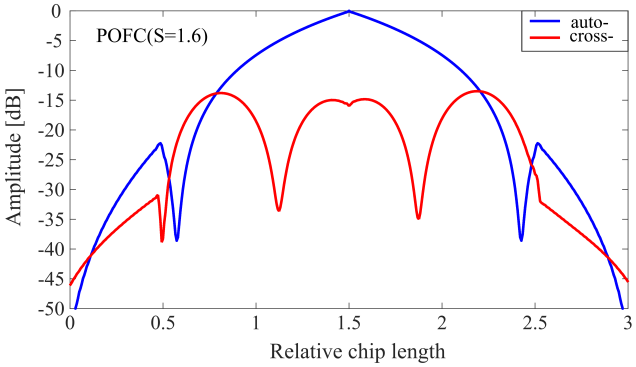

Fig. 5. COM simulation of auto- and cross-correlation of POFC (S = 1.6). The time axis is normalized with chip length τ_{chip}. The peak value of the cross-correlation is approximately −13 dB.

For an average of 50 electrodes for each reflector, Fig. 4 and Fig. 5 show the auto- and cross-correlation between adjacent frequencies using OFC and POFC (S = 1.6), respectively. The results show that the maximum cross-correlation of adjacent frequencies is approximately −9 dB and −13 dB, respectively.

3. Mixed-POFC

3.1. The theory of Mixed-POFC

To take both overlap and coding diversity into consideration, a Mixed-POFC method is proposed in this study. In this method, the center frequencies of the OFC chips are chosen in an alternating fashion from f_1 to f_7. Chips can be divided into two groups (a first group of f_1, f_3, f_5, f_7, and a second group of f_2, f_4, f_6). Both center frequency groups are fully used in our proposed Mixed-POFC unlike in POFC in which only one center frequency group is applied. For a 7-chip Mixed-POFC system, the spectrum utilization rate is better than the 7-chip POFC system with S = 1.6, shown in Fig. 2 and Fig. 3. Figure 6 shows the auto- and cross-correlation with adjacent frequencies using Mixed-POFC for an average of 50 electrodes for each reflector, where the peak cross-correlation of adjacent frequencies is lower than −15 dB.

It is found that the cross-correlation of the Mixed-POFC is lower than that of pseudo-OFC by comparing Fig. 5 and Fig. 6.

The chips have two arrangement modes marked as single-track and dual-track in the Mixed-POFC method as shown in Fig. 7 and Fig. 8. In Fig. 7, chips of the same group are arranged in the single track. Alternatively, the two groups of chips can also be ar-

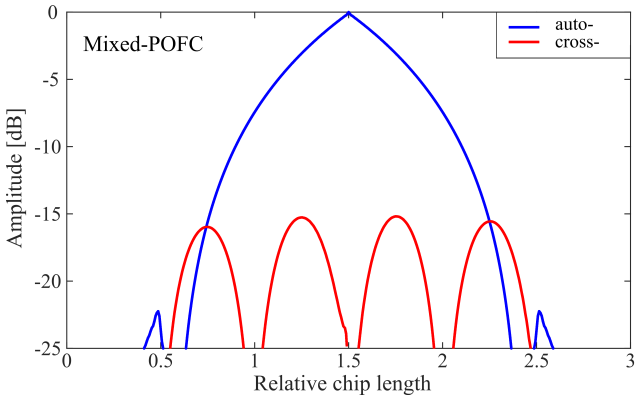

Fig. 6. COM simulation of auto- and cross-correlation of reflector chips with 50 electrodes of Mixed POFC. The time axis is normalized by the chip length τ_{chip}. The peak value of the cross-correlation is lower than −15 dB.

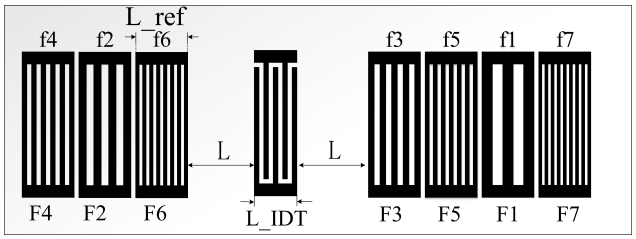

Fig. 7. Schematic of the 7-chip Mixed-POFC tag.

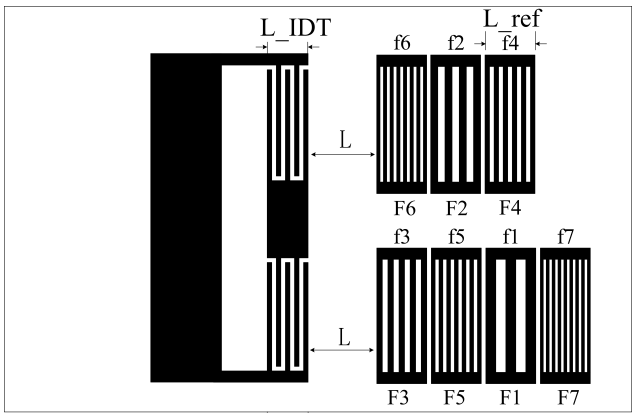

Fig. 8. Schematic of the 7-chip Mixed-POFC tag with a dual track.

ranged in a dual track as shown in Fig. 8. In addition, the frequency spacing factor in these two structures is the same with $S = 2$.

The main difference between the two arrangements in Fig. 7 and Fig. 8 is the minimum length of the chip. The IDT and chips are usually placed on a line, such as the arrangement in Fig. 1, for traditional SAW RFID tag structure. For a 7-chip Mixed-POFC system, the cost of the structure shown in Fig. 7 is not higher than that of Fig. 1. As shown in Fig. 8, the length of the device is shorter than that in Fig. 7. Thus, the structure of Fig. 8 is more suitable for some special applications with a length limit on the SAW tag. The transfer function of the two track arrangement is the same, which means the calculation is the same.

The SAW signal is transmitted through both directions of the IDT. Chips with different center frequencies have a different electrode cycle, though the chip length is same. Chips are placed on two sides of the IDT. The distance from the IDT to the chips on each side is the same. F1, F2, F3, F4, F5, F6 and F7 are marked as the numbers of the reflectors corresponding to each center frequency.

The SAW signal is transmitted in one direction. The distance from the IDT to chips in the upper and lower groups is the same. The reflected signals are overlapped in the receiver terminal. F1, F2, F3, F4, F5, F6 and F7 are the numbers of the reflectors corresponding to each center frequency.

The following work is based on the structure in Fig. 7. The transfer function can be shown as the sum of two groups of chips. The peak value of the cross-correlation is lower than −15 dB (Smith, 1977). For a special two-chip Mixed-POFC,

$$\tau_{p_m} = \tau_{p_n} = 0, \tag{8}$$

where τ_p is the delay of each chip from the transducer, m and n are orthogonal frequencies from the two groups of chips which have the same distance to IDT. Equation (1) can be expanded to produce the transfer function of the sum of orthogonal sinc function in frequency. In the time domain, the transfer function is given as:

$$h_{\cos}(t) = \cos\left(\frac{2\pi kt}{2\tau_{\text{chip}}}\right)\cos\left[\frac{2\pi\tau(f_{\text{chip}_m} + f_{\text{chip}_n})}{2}\right] \cdot \text{rect}\left(\frac{t}{\tau_{\text{chip}}}\right), \tag{9}$$

$$\tau_{\text{chip}} = \frac{k}{f_{\text{chip}_m} - f_{\text{chip}_n}}, \tag{10}$$

where $k = m - n$

The cosine-envelope waveform with a center frequency of $f_c = k/2\tau_{\text{chip}}$ has different wavelengths according to the choice of k. The number of half wavelengths shown in the window can only be odd due to the window function and the characteristic of k.

For the 7-chip Mixed-POFC system mentioned, there are 3 values of k exist ($k = 1, 3, 5$) corresponding to only three different cosine envelopes. A change in the k parameter causes a change in the envelope waveform, as shown in Fig. 9.

The left column of Fig. 9 shows the newly constructed waveform in the time domain, while the right column shows the overlap in the frequency domain caused by the signal in the left diagram. The quantity of half wavelength in each cosine envelope is changed due to the different k values, as shown in the left column.

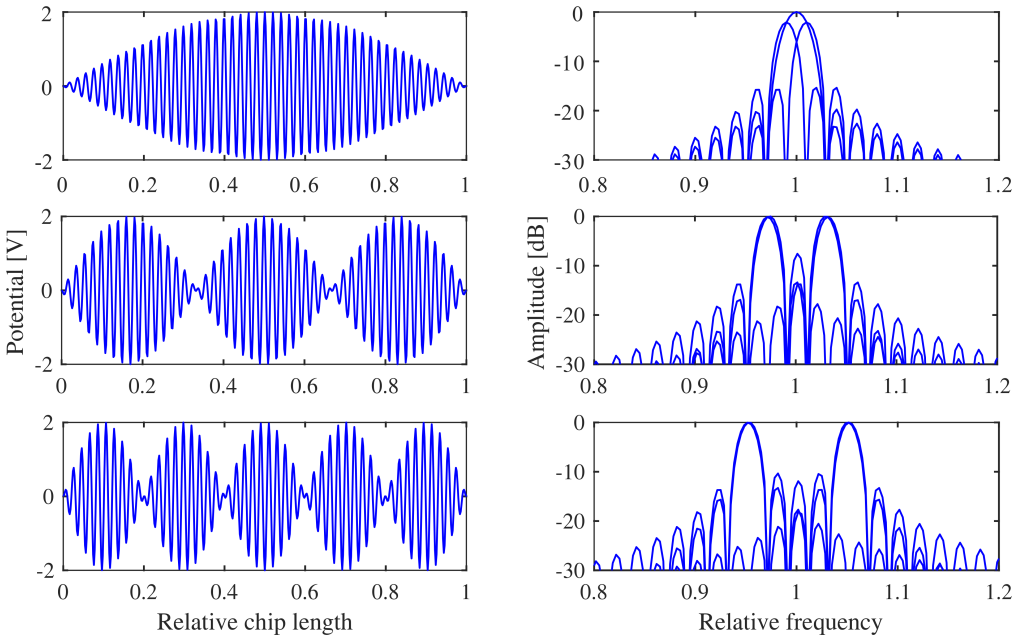

Fig. 9. The cosine-envelope waveform response of two orthogonal chips.

3.2. Example of Mixed-POFC RFID and FEA result

3.2.1. Model parameter

A 7-chip Mixed-POFC SAW tag system is set up as shown in Fig. 7. The device operates at a center frequency of 336 MHz on YZ-$LiNbO_3$. There are 50 electrodes on average for each reflector. To have the same chip length according to Eq. (2), chips with different center frequencies have different electrode cycles. As shown in Fig. 7, the reflector code sequences for this device are F4, F2, F6, F3, F5, F1, and F7; the group of frequencies including f_3, f_5, f_1, and f_7 are placed on the right side of IDT, and the others (f_4, f_2, f_6) are placed on the left.

The simulation model is established by COM and FEA. The electrode number of IDT and reflectors are shown in Table 1, The wavelength and design frequency of the IDT and reflectors are calculated by the COM model. The frequency indices of each reflector correspond to the reflectors shown in Fig. 10. More details of the model are in Table 1. The Mixed-POFC device has a bandwidth of interest from 315.9 MHz to 356.3 MHz, a frequency span of 40.4 MHz, and a fractional bandwidth of 12.8% at a 336 MHz center frequency.

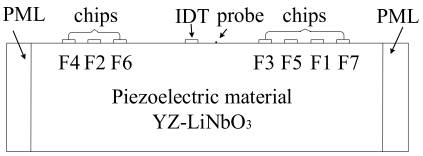

Fig. 10. A simplified 2D model of the 7-chip Mixed-POFC tag established by the software COMSOL Multiphysics.

There is a direct comparison between Mixed-POFC and POFC under the same fractional bandwidth of 12%. By using Mixed-POFC, the coding diversity increases to 4!3! = 144; for POFC, the coding number is only 5! = 120, and the fractional bandwidth is 12.8% (a bit wider than Mixed-POFC) for an S parameter of 1.6. If S = 2.4, the situation can be even worse: the coding number is only 3! = 6 (fractional bandwidth of 9.6%). If the limit on bandwidth is broadened, coding can be 5! = 20 (fractional bandwidth of 19.2%). The conclusion can be drawn that Mixed-POFC has more coding diversity than POFC with the same fractional bandwidth.

Table 1. Details of the 7-chip Mixed-POFC tag.

	IDT	F1	F2	F3	F4	F5	F6	F7
Number of electrodes	20	47	48	49	50	51	52	53
Wavelength [μm]	10	10.638	10.417	10.204	10	9.803	9.615	9.434
Designed frequency [MHz]	341.8	315.9	322.7	329.4	336.1	342.8	349.6	356.3
Frequency index	–	1	2	3	4	5	6	7
Length of chip [μm]	100	250	250	250	250	250	250	250

3.2.2. FEA result

To obtain the frequency properties of the Mixed-POFC system, a 2D model of a 7-chip Mixed-POFC tag system is established using COMSOL Multiphysics software (Yantchev *et al.*, 2016; Salim *et al.*, 2016). A schematic of the 7-chip Mixed-POFC tag is shown in Fig. 10. The reflectors are placed on the two sides of the IDT (single track). The material of the IDT and reflectors is aluminum, while the piezoelectric material is YZ-$LiNbO_3$. PML is a perfect matching layer. There is a probe located one third of the distance between the IDT and chip F3, close to the IDT. Parameters of electrodes, wavelength, chip length and frequency and frequency value are listed in Table 1. In this structure, the SAW signal is transmitted in both directions from the IDT. The distances from the IDT to the chips on both sides are the same. The reflected signals are overlapped in the receiver terminal, which is the probe between the IDT and chip F3.

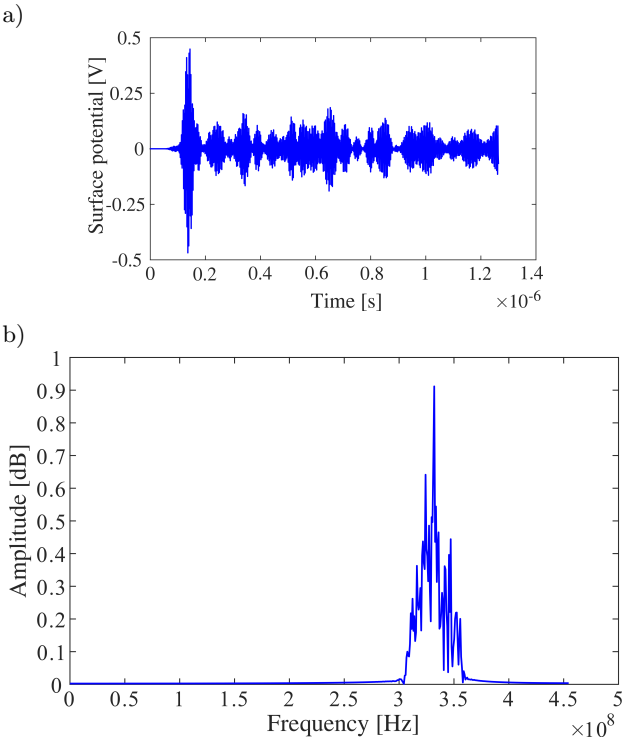

Fig. 11. a) Time and b) frequency responses of the 7-chip Mixed-POFC tag detected by the probe located at one-third of the distance between IDT to F3.

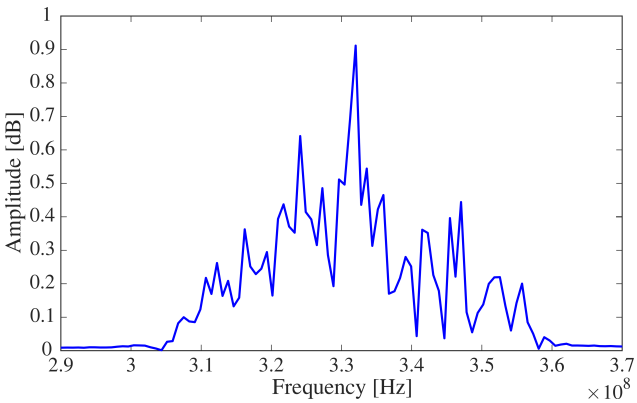

Fig. 12. The seven peak frequencies correspond to the seven reflectors of different center frequencies.

The time and frequency responses of the 7-chip Mixed-POFC tag detected by the probe are shown in Fig. 11. The main frequency information is focused in the range between 300 MHz to 360 MHz as shown in Fig. 11b, and Fig. 12 shows the frequency responses in this range. The seven peak frequencies correspond to the seven reflectors of different center frequencies.

The frequency information is extracted from the time response using an FFT and shown in Table 2. For the seven reflectors, the absolute error and relative error between the designed frequency and the simulation frequency is calculated. Figure 13 shows a comparison between designed frequency and simulation frequency.

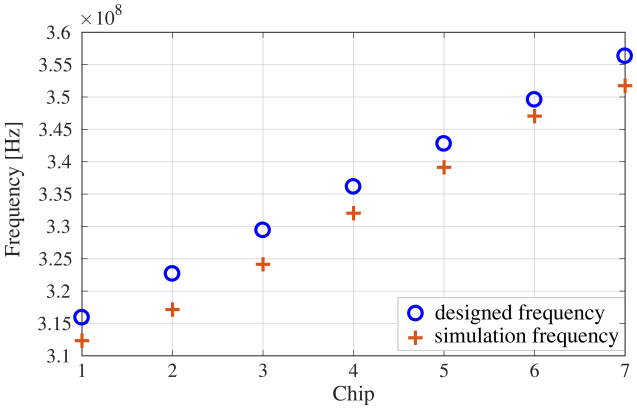

Fig. 13. A comparison of the designed and simulation frequency for the seven reflectors, the maximum error between the designed and simulation frequency is 1.7%.

Table 2. The designed and simulation frequency for each reflector.

	F1	F2	F3	F4	F5	F6	F7
Frequency index	1	2	3	4	5	6	7
Wavelength [μm]	10.638	10.417	10.204	10	9.803	9.615	9.434
Designed frequency [MHz]	315.9	322.7	329.4	336.1	342.8	349.6	356.3
Simulation frequency [MHz]	312.3	317.1	324.1	332.0	339.1	347.0	351.8
Absolute error [MHz]	3.6	5.6	5.3	4.1	3.7	2.6	4.5
Relative error	1.1%	1.7%	1.6%	1.2%	1.1%	0.7%	1.3%

The results show that the maximum error between the designed and simulation frequency is 1.7%, which demonstrates the coding method of Mixed-POFC is practicable.

4. Conclusion

This paper proposes a Mixed-POFC method that allows the responses of chips to overlap in time while increasing the coding diversity. The method can also improve the utilization of spectrum. The auto- and cross-correlation are calculated to quantify the reduction of overlap in the frequency domain for two chips. The advantages in coding diversity and spectrum utilization for Mixed-POFC are demonstrated by the coding number comparison between 7-chip Mixed-POFC and 7-chip POFC.

To use the Mixed-POFC method, the SAW tag is designed with multi-track chip arrangements. A 2D model of a 7-chip Mixed-POFC tag system is established in COMSOL software to analyze the frequency characteristics. The maximum error between designed frequencies and simulation frequencies is only 1.7%, which suggests that the Mixed-POFC technique is promising.

Acknowledgments

The authors are grateful to the support of and the National Science Foundation of China (Grant No. 61571319).

References

1. Gallagher M.W., Malocha D.C. (2013), *Mixed orthogonal frequency coded SAW RFID tags*, IEEE Transactions on Ultrasonics, Ferroelectrics and Frequency Control Journal, **60**, 3, 596–602.
2. Humphries J.R., Gallagher M.W., Gallagher D.R., Weeks A.R., Malocha D.C. (2015), *Interrogation of orthogonal frequency coded SAW sensors using the USRP*, [in:] Proceedings of the 2015 Joint Conference of the IEEE International Frequency Control Symposium the European Frequency and Time Forum; Denver, Co, USA, April 12–16, 2015; pp. 530–535.
3. Humphries J.R., Malocha D.C. (2015), Wireless SAW strain sensor using orthogonal frequency coding, IEEE Sensors Journal, **15**, 10, 5527–5534.
4. Liu W., Xing J., Xie L. (2016), *Matrix method for multiple wireless orthogonal frequency-coded SAW sensor tags identification*, IEEE Sensors Journal, **16**, 10, 3834–3847.
5. Malocha D., Puccio D., Gallagher D. (2004), *Orthogonal frequency coding for SAW device applications*, [in:] Proceedings of IEEE Ultrasonics Symposium, August 23–27, 2004 Montreal, Canada, Vol. 2, pp. 1082–1085.
6. Malocha D.C., Fisher B., Youngquist R., Weeks A. (2014), *Surface acoustic wave pulsed-correlator transceiver for aerospace applications*, IEEE Sensors Journal, **14**, 11, 3775–3781.
7. Plessky V.P., Kondratiev S.N., Stierlin R., Nyffeler F. (1995), *SAW-tags: New ideas*, [in:] Proceedings of IEEE Ultrasonics Symposium, November 7–10, 1995, Seattle, Washington, Vol. 1, pp. 117–120.
8. Puccio D., Malocha D.C., Gallagher D., Hines J. (2004), *SAW sensors using orthogonal frequency coding*, [In:] Proceedings of IEEE International Frequency Control Symposium, August 23–27, Montreal, Canada, pp. 307–310.
9. Rodriguez L.M., Gallagher D.R., Gallagher M.W., Fisher B.H., Humphries J.R., Malocha D.C. (2014), *Wireless SAW sensor temperature extraction precision*, IEEE Sensors Journal, **14**, 11, 3830–3837.
10. Saldanha N., Malocha D. (2008), *Low loss SAW RFID tags for space applications*, [in:] Proceedings of IEEE Ultrasonics Symposium, November 2–5, Beijng, China, pp. 292–295.
11. Saldanha N., Malocha D.C. (2012), *Pseudo-orthogonal frequency coded wireless SAW RFID temperature sensor tags*, IEEE Transactions on Ultrasonics, Ferroelectrics and Frequency Control Journal, **59**, 8, 1750–1758.
12. Salim Z.T., Hashim U., Arshad M.K. (2016), *FEM modeling and simulation of a layered SAW device based on ZnO/128° YX $LiNbO_3$*, [in:] Proceedings of 2016 IEEE International Conference on Semiconductor Electronics, August 17–19, Kuala Lumpur, Malaysia, pp. 5–8.
13. Smith W. (1977), *SAW Filters for CPSM spread spectrum communication*, [in:] Proceedings of IEEE International Ultrasonics Symposium, October 26–28, Arizona, USA, pp. 524–528.
14. Stremler F.G. (1990), *Introduction to communication systems*, Addison-Wesley, Reading, Ma.
15. Wilson W. *et al.* (2009), *Orthogonal frequency coded SAW sensors for aerospace SHM applications*, IEEE Sensors Journal, **9**, 11, 1546–1556.
16. Yantchev V., Turner P., Plessky V. (2016), *COMSOL modeling of SAW resonators*, IEEE International Ultrasonics Symposium, September 18–21, Tours, France, pp. 1–4.